ISSN 0021-3640, JETP Letters, 2026, Vol. 123, No. 7, pp. 433–443. © The Author(s), 2026. This article is an open access publication.
Russian Text © The Author(s), 2026, published in Pis'ma v Zhurnal Eksperimental'noi i Teoreticheskoi Fiziki, 2026, Vol. 123, No. 7, pp. 443–453.

ASTROPHYSICS, SPACE PHYSICS, COSMOLOGY, AND GRAVITY

Indications of Electron-to-Proton Mass Ratio Variations in the Galaxy. III. 0.6 mm Methanol Lines Toward Sgr B2(N) and Orion-KL

J. S. Vorotyntseva[a],* and S. A. Levshakov[a]

[a] *Ioffe Institute, St. Petersburg, 194021 Russia*

**e-mail: j.s.vorotyntseva@mail.ioffe.ru*

Received February 2, 2026; revised February 27, 2026; accepted February 28, 2026

In this paper, we show that methanol (CH_3OH), torsional-rotational transitions, which have increased sensitivity to small variations of the electron-to-proton mass ratio μ, are shifted relative to less sensitive transitions in the spectrum of the Sgr B2(N) molecular cloud located at the Galactic center. At the same time, an identical set of methanol lines in the spectrum of the Orion-KL molecular cloud, located far from the center, shows no shifts. Interpreting this behavior of molecular frequencies in terms of $\Delta\mu/\mu = (\mu_{obs} - \mu_{lab})/\mu_{lab}$ leads to the following weighted mean values: $\langle\Delta\mu/\mu\rangle = (-3.4 \pm 0.4) \times 10^{-7}$ for Sgr B2 and $\langle\Delta\mu/\mu\rangle = (-1.1 \pm 0.8) \times 10^{-7}$ for Orion-KL (indicated are the total $\pm 1\sigma$ errors of the weighted means $\langle\Delta\mu/\mu\rangle$ including both statistical and systematic uncertainties). A possible correlation between $\Delta\mu/\mu$ values measured in various molecular clouds of the Galactic disk and the distribution of dark matter along the Galactic radius is discussed, which may suggest a hypothetical modulation of the Higgs scalar field by dark matter, resulting in a change of μ.

DOI: 10.1134/S0021364026600345

1. INTRODUCTION

Complex organic molecules such as methanol (CH_3OH), ubiquitous in molecular clouds that fill the Galactic disk from the circumnuclear regions with galactocentric distances of $R_{GC} \lesssim 100$ pc, like Sagittarius (Sgr) B2 [1, 2], to the periphery ($R_{GC} \lesssim 23$ kpc [3, 4]) are convenient probes not only of the physical conditions in star-forming regions, but also a unique tool in the search for new physics (see, e.g., the review [5]). The special role of methanol in these tasks is explained by three factors: (i) the frequencies of torsional-rotational transitions in CH_3OH exhibit high sensitivity to small variations in the electron-to-proton mass ratio $\mu = m_e/m_p$ [6, 7]; (ii) the methanol line spectrum fills a broad frequency range from GHz to THz, accessible to observations with modern ground-based and orbital telescopes; (iii) the methanol lines are sufficiently intense to provide high-quality spectra with a high signal-to-noise ratio.

Let us now explain what is meant by the term "New Physics." According to Einstein's Equivalence Principle (EEP) and its fundamental component, the Local Position Invariance (LPI), the results of non-gravitational experiments should be independent of spatial and temporal coordinates. The detection of deviations from the LPI in laboratory experiments with atomic and nuclear clocks and/or in astrophysical spectral observations would mean the manifestation of new physical laws that go beyond the Standard Model of particle physics. A violation of the EEP is assumed in various chameleon scenarios of the screening of the fifth force, in multidimensional models, in models of the dark sector (dark matter, DM, and dark energy, DE) and in a number of other theories, considered, for example, in the review [8].

In practical tasks of searching for New physics, spectral lines of various chemical elements are widely used, since the structure of the energy levels of atoms and molecules depends on the values of fundamental physical constants, which, if the LPI is violated, would change their values, thereby causing shifts in the corresponding frequencies. In particular, small changes in the constant μ would lead to significant shifts in the frequencies of tunnel transitions in molecules such as NH_3, CH_3OH, etc. [5, 9–12].

The masses of elementary particles (an electron and three quarks), on which the ratio m_e/m_p depends, are in turn modulated by the Higgs scalar field. However, the proton mass (938 MeV/c^2) is determined mainly by the binding energy of three quarks, the total mass of which (~10 MeV/c^2) is approximately 1% of the total mass of the proton. Therefore, it can be assumed that, first of all, the variations of μ should have been associated with a change in the electron

mass, which is given as the product of the Yukawa coupling constant for the electron $\lambda_e \approx 2.9\times10^{-6}$ and the mass of the Higgs boson v (~246 GeV): $m_e = \lambda_e v/\sqrt{2}$ [13].

The cosmological evolution of the Higgs boson mass v in the expanding Universe, and hence the dependence of μ on cosmological time, was considered, for example, in [13]. The question we will attempt to answer in this paper is the local behavior of μ, namely, whether there is any correlation between the local dark matter density ρ_{DM} and the measured value of $\Delta\mu/\mu = (\mu_{obs} - \mu_{lab})/\mu_{lab}$ in the Galactic disk.

In the Galaxy, as is well known, with increasing R_{GC} the ratio ρ_{br}/ρ_{DM} changes significantly: the density of the baryon component ρ_{br} sharply decreases with increasing R_{GC}, while ρ_{DM} increases [14–18]. Both densities equalize at approximately two effective radii, (R_{eff}),[1] after which dark matter becomes the dominant component of the Galactic disk and halo.

Limits on the variations of μ far from the Galactic center ($R_{GC} \geq R_{eff}$) were previously established using different methods. The tightest limits were obtained at the level of $\Delta\mu/\mu < (1–4)\times10^{-8}$ [10–12, 22–25]. The Galactic center remained unexplored until recently.

First attempts to estimate $\Delta\mu/\mu$ using three methanol transitions at frequencies ~540 GHz (observations of the Herschel[2] space telescope), and also eleven methanol lines from the 3 mm atmospheric window (observations with the 30-m IRAM[3] telescope) showed a possible decrease in μ in the molecular complex Sgr B2(N): $\Delta\mu/\mu = (-4.2 \pm 0.7)\times10^{-7}$ [26] and $\Delta\mu/\mu = (-2.1 \pm 0.6)\times10^{-7}$ [27], respectively.

In this paper, we continue our studies in the high-frequency range (490–640 GHz) based on observations by the Herschel space telescope in two directions: toward the Galactic Center, the Sgr B2(N) molecular complex, and, for control, toward an object localized far from the Galactic center at a distance of R_{GC} ~ 9 kpc—the Orion-KL molecular complex. The new analysis was performed on an expanded sample of methanol lines compared to [26]: ten new lines, selected from each of the Herschel spectra of these two objects, were added to the three previous lines.

[1] The effective radius (R_{eff}) is defined as the length of the semi-major axis of the elliptical isophote, which includes half the light of the galaxy's stellar component. For the Galaxy, $R_{eff} \approx 4.5$ kpc, and the galactocentric distance of the solar system $R_{Sun} \approx 1.8R_{eff}$ [19–21].

[2] Herschel is an ESA space observatory, equipped with instruments developed by leading European centers with significant participation from NASA.

[3] The Institute for Radio Astronomy in the Millimeter Range (IRAM) is an international research institute and Europe's leading center for radio astronomy.

2. PARAMETERS OF HERSCHEL OBSERVATIONS

In this work, the archival spectra of the Herschel space observatory, obtained in the direction of two molecular complexes—Sgr B2(N) and Orion-KL, are used. Both objects belong to active star formation zones with masses and linear sizes $M_{SgrB2(N)} \sim 2\times10^3 M_{Sun}$, $D_{SgrB2(N)} \sim 0.2$ pc [29] and $M_{Ori\text{-}KL} \sim 2\times10^2 M_{Sun}$, $D_{Ori\text{-}KL} \sim 0.02$ pc [30].

A description of the equipment used to obtain the spectra, as well as information about the primary processing of the spectra, is given in our work [26]. Here we report only the main technical characteristics listed in Table 1: observed frequency ranges, corresponding spectral bands, telescope guidance coordinates (right ascension and declination), dates of observations, aperture sizes θ_{HPBW} and spectral resolution Δ_{ch}.

Among the spectra corresponding to these ranges, there are a number of methanol CH_3OH lines observed in both Sgr B2(N) and Orion-KL, which are most suitable for estimates of $\Delta\mu/\mu$. The selection criteria for such lines are as follows: (1) a sufficient signal-to-noise ratio of $SNR \geq 40$; (2) lines falling into the same IF band (4 GHz); (3) close values of the energies of the upper levels E_u; (4) different sensitivity coefficients Q (see Table 2) to small variations of μ ($|\Delta Q| > 0$); (5) known laboratory frequency f_{lab}. This selection and distribution of lines across sub-ranges is chosen to avoid possible systematic errors associated with the calibration of the frequency and temperature scales. First of all, the calibration error of the frequency scale is eliminated, which can be significant for different IF bands and different spectral ranges. Another source of instrumental errors is different observation dates and different aperture sizes. Also, the selected lines do not fall into the marginal regions of the spectral band in order to avoid the known "accordion effect"—changes of channel widths at the edges of the spectral range. The median error of calibration of the frequency scale within the IF band does not exceed 50 kHz [35]. The temperature scale (T_A) was calibrated with an accuracy of 1.6–4% in band 1 and 1.3–3% in band 2 (see Tables 5, 6 in [32]).

The parameters of the methanol transitions selected in this way are summarized in Table 2: the first column shows the line number, the second—quantum numbers—the total angular momentum J and its projection onto the axis of symmetry of the molecule K for the upper u and lower ℓ levels, the third column lists the energies of the upper levels E_u, taken from [33], the fourth and fifth columns display the laboratory frequencies f_{lab} [33] and the calculated frequencies f_{cal} [34], respectively. The values of the sensitivity coefficients Q [7] are given in the last column.

Table 1. Characteristics of observations and coordinates of the objects [1, 31]. The second column shows the frequency ranges Δf, in which the methanol lines CH_3OH were selected. The corresponding observed frequency bands have the following values: 479.5–561.5 GHz (*band 1a*), 554.5–635.5 GHz (*band 1b*) and 626.0–726.0 GHz (*band 2a*). Telescope aperture θ_{HPBW} (Half Power Beam Width) in the center of the band and spectral resolution Δ_{ch} (channel width) are given in the fifth and sixth columns. For all three spectral ranges, the width of the intermediate frequency band (IF) is equal to 4 GHz [1, 32]

Target	Frequency range, Δf	Coordinates (J2000)	Observation date	θ_{HPBW} (″)	Δ_{ch} (km s^{-1})
Sgr B2(N)	493–496 GHz 541–544 GHz (*band 1a*)	$17^h47^m20^s.06$ −28°22′18″.33	22.09.2010	40.4	0.3
	589–591 GHz (*band 1b*)	$17^h47^m20^s.04$ −28°22′18″.29	12.10.2010	35.3	0.25
	637–639 GHz (*band 2a*)	$17^h47^m19^s.55$ −28°22′18″.33	15.09.2010	31.1	0.23
Orion-KL	493–496 GHz 541–544 GHz (*band 1a*)	$05^h35^m14^s.36$ −05°22′33″.63	01.03.2010	40.4	0.3
	589–591 GHz (*band 1b*)	$05^h35^m14^s.35$ −05°22′33″.06	02.03.2010	35.3	0.25
	637–639 GHz (*band 2a*)	$05^h35^m14^s.32$ −05°22′32″.91	12.04.2010	31.1	0.23

Table 2. Parameters of the selected methanol lines CH_3OH. The measured laboratory f_{lab} and calculated f_{cal} line frequencies (in MHz) are taken, respectively, from [33] and [34]. The energies of the upper torsion-rotational levels E_u are indicated in the third column. The values of the sensitivity coefficients Q are calculated in [7], where $K_\mu = -Q$. The uncertainties of 1σ in the last digits are given in parentheses

No.	Transition $J_{K_u} \to J_{K_\ell}$	E_u (K)	Measured frequencies, f_{lab}	Calculated frequencies, f_{cal}	Q
1	$5_3 \to 4_2A^+$	84.6	493699.095(50)	493699.112(15)	−0.1
2	$5_3 \to 4_2A^-$	84.6	493733.672(50)	493733.687(15)	−0.1
3	$7_2 \to 7_1A^{-+}$	102.7	494481.683(50)	494481.555(12)	1.5
4	$7_0 \to 6_{-1}E$	78.0	495173.104(50)	495173.105(12)	1.8
5	$6_3 \to 5_2A^+$	98.5	542000.981(50)	542000.954(14)	0.0
6	$6_3 \to 5_2A^-$	98.5	542081.936(50)	542081.952(14)	0.0
7	$8_0 \to 7_{-1}E$	96.6	543076.194(50)	543076.175(12)	1.7
8	$7_3 \to 6_2A^+$	115.0	590277.688(50)	590277.712(14)	0.1
9	$7_3 \to 6_2A^-$	114.7	590440.291(50)	590440.430(14)	0.1
10	$9_0 \to 8_{-1}E$	117.4	590790.957(50)	590790.939(12)	1.6
11	$10_0 \to 9_{-1}E$	140.5	638279.564(50)	638279.651(12)	1.6
12	$8_3 \to 7_2A^+$	133.3	638523.486(50)	638523.509(13)	0.1
13	$8_3 \to 7_2A^-$	133.3	638817.830(50)	638817.824(13)	0.1

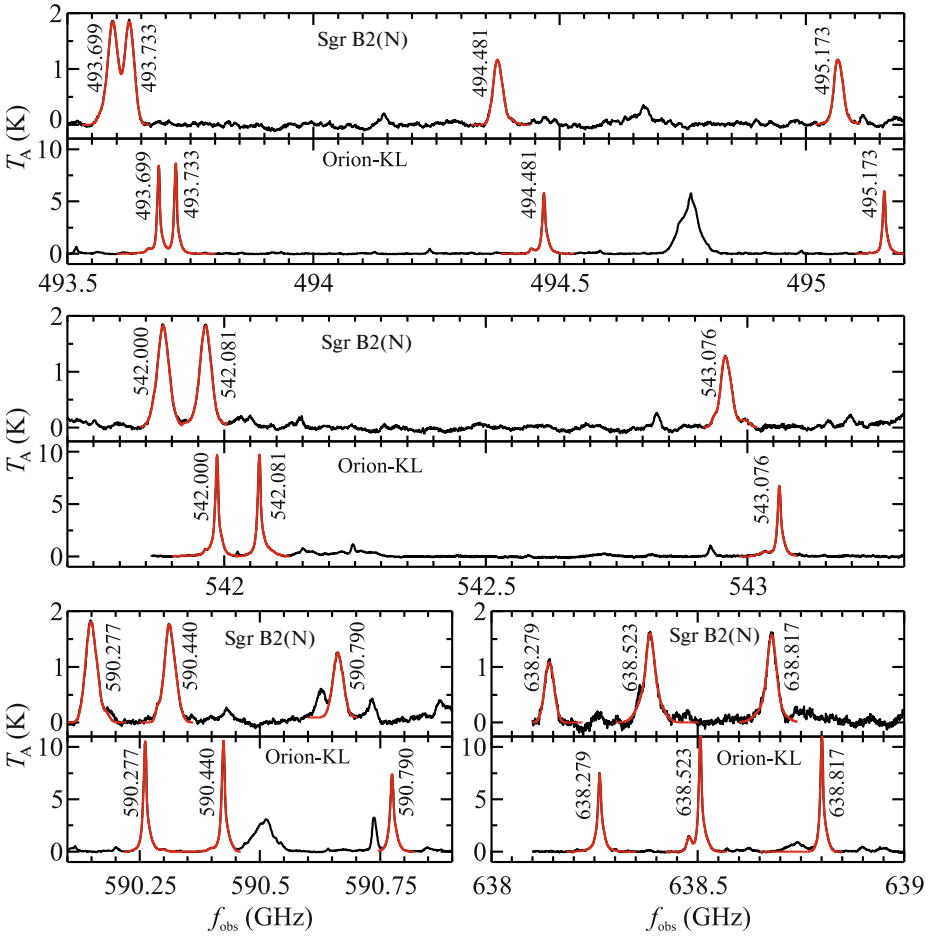

Fig. 1. (Colored online) The methanol (CH_3OH) lines toward two sources—Sgr B2(N) and Orion-KL, obtained at the space observatory Herschel. The original spectra are shown in black and the model spectra—in red. The numbers next to the lines indicate laboratory frequencies f_{lab} in GHz (see Table 2).

3. SPECTRA PROCESSING AND CALCULATED LINE PARAMETERS

The processing of the spectra consisted of describing the shape of the profile of the observed line using an envelope curve and determining its center; i.e., the point at which the envelope reaches its maximum. For this purpose, we used a set of Gaussians with the minimum number of components, which provided the value $\chi^2_\nu \le 1$, where ν is the number of degrees of freedom.

The envelope curves calculated in this way are shown in Fig. 1 in red and the original spectra—in black. An object and the laboratory frequencies of the observed lines are signed for each spectrum.

The calculated parameters of the methanol lines from the Sgr B2(N) spectrum are listed in Table 3: serial number of the line (according to Table 2)—in the first column, the observed frequency (measured center of the line) f_{obs}—in the second column with the designation of the type of molecule—A or E, the third and fourth columns show the widths *FWHM* of the lines and the observed peak temperatures of the main antenna beam T_A^{peak}, respectively, the radial velocities $V_{LSR}^{(k)}$ are given in the fifth and sixth columns which are calculated in accord with the radio astronomical convention:

$$V_{LSR}^{(1)} = c\left(1 - f_{obs}/f_{lab}\right), \quad V_{LSR}^{(2)} = c\left(1 - f_{obs}/f_{cal}\right). \quad (1)$$

The line width errors are ~5%, taking into account the contribution from the uncertainty of the flux calibration and the contribution from the measurement errors of the line widths from the observed spectra. The uncertainties of peak temperatures include the statistical component—the average local noise amplitude (rms) near the methanol line under consideration—and the systematic—majority error of the temperature scale calibration (see Section 2). Both contributions were added up quadratically. The radial velocity uncertainties were calculated from the statistical error of determining the center of the line $\sigma_{f_{obs}}$, ref-

Table 3. Parameters of the observed methanol lines in the Sgr B2(N) spectrum—center frequency f_{obs}, full line width at half maximum *FWHM* and the peak intensity in the center of the line T_A^{peak}.The lines are numbered according to Table 2. $V_{LSR}^{(1)}$ and $V_{LSR}^{(2)}$ are the radial velocities calculated using measured laboratory frequencies f_{lab} and predicted in theoretical calculations f_{cal}, respectively (see Table 2). The 1σ errors in the last digits are shown in parentheses. The error in the *FWHM* is 5%

No.	f_{obs} (MHz)	*FWHM* (km s^{-1})	T_A^{peak} (K)	$V_{LSR}^{(1)}$ (km s^{-1})	$V_{LSR}^{(2)}$ (km s^{-1})
1	493592.41(50) A	15	1.85(8)	64.78(30)	64.79(30)
2	493625.81(50) A	14	1.85(8)	65.49(30)	65.50(30)
3	494 373.85(10) A	14	1.16(5)	65.38(7)	65.30(7)
4	495064.98(7) E	13	1.16(5)	65.46(6)	65.47(5)
5	541 883.19(6) A	15	1.83(8)	65.15(5)	65.14(4)
6	541 964.24(6) A	14	1.82(8)	65.09(5)	65.10(4)
7	542957.84(8) E	13	1.27(6)	65.34(6)	65.32(5)
8	590 148.89(6) A	14	1.81(8)	65.41(5)	65.43(4)
9	590 311.39(6) A	13	1.76(8)	65.45(5)	65.52(4)
10	590 661.67(9) E	13	1.24(6)	65.61(6)	65.60(5)
11	638 140.50(20) E	13	1.08(7)	65.32(10)	65.36(10)
12	638 384.62(18) A	14	1.60(8)	65.20(9)	65.21(9)
13	638679.10(17) A	13	1.57(8)	65.11(9)	65.10(8)

erence frequency errors $\sigma_{f_{lab}}$, as well as from the median calibration error of the frequency scale, 50 kHz [35]. The statistical uncertainties $\sigma_{f_{obs}}$ were calculated using the $\Delta\chi^2$ method [36], taking into account the correlation of noise in the spectra.

The correction factor $\gamma \sim 1.15$ (Eq. (5) in [27]) slightly adjusted the noise amplitude $\sigma_{rms}^{cor} = \gamma\sigma_{rms}$. This method of calculating the statistical error is justified, since the calculated values $\sigma_{f_{obs}}$ match with good accuracy the expected values, which are expressed in terms of channel width Δ_{ch}, the full line width *FWHM* and the signal-to-noise ratio *SNR* (see formula (8) and Table 3 in [26]).

The exception is lines *1* and *2* from the Sgr B2(N) spectrum, which turned out to be partially resolved (see Fig. 1). The wings of these lines influence the definition of the envelope centers, shifting them either to the left (line *1*) or to the right (line *2*) by almost the channel width relative to the mean value $V_{LSR} = 65.138$ km s^{-1}, despite the fact that both lines have the same sensitivity coefficients $Q = -0.1$. Similar lines in the Orion-KL spectrum, where there is no wing overlap, show the same radial velocities (see Table 4). Therefore, we increased the errors of lines *1* and *2* in the Sgr B2(N) spectrum to the channel width $\Delta_{ch} = 0.3$ km s^{-1}. In all other cases, the resulting radial velocity error is calculated as the quadratic sum of the errors $\sigma_{f_{obs}}$, $\sigma_{f_{lab}}$ and systematic error $\sigma_{f_{sys}} = 50$ kHz, which were discussed above.

Before proceeding directly to the estimates of $\Delta\mu/\mu$, which are obtained from various combinations of A- and E-methanol lines, it is necessary to analyze the measured sequence of peak temperatures to determine the physical conditions under which this sequence could form. This question arises due to the fact that direct radiation or collision processes are prohibited between A- and E-methanol, and the A/E abundance ratio in the molecular cloud practically does not change from the moment of formation of the molecules. At the same time, the formation of methanol in a cold gas at $T_{kin} = 10$–15 K leads to an overabundance of A-methanol, but in a warm or hot gas at $T_{kin} \geq 40$ K the A/E ratio is aligned [37]. Therefore, in some cases, these two forms of methanol are considered as two molecules and it needs to be checked whether they trace the same gas.

Peak temperatures from Table 3 were checked using the RADEX code [38], which calculates the radiation transfer in molecular lines when deviating from local thermodynamic equilibrium (non-LTE). A model of a homogeneous plane-parallel layer was used, which most closely describes the observed intensities of the methanol lines. We took the temperature of the background radiation as $T_{bg} = 2.73$ K, and as the line width is the median value from Table 3, *FWHM* = 14 km s^{-1}. The collision rates with H_2 are known with an error of 3% [39], which was taken into account when comparison of the calculated peak temperatures with the observed ones. It turned out that the observed sequence of peak temperatures can be

Table 4. Same as Table 3, but for the observed methanol lines in the Orion-KL spectrum

No.	f_{obs} (MHz)	*FWHM* (km s^{-1})	T_A^{peak} (K)	$V_{LSR}^{(1)}$ (km s^{-1})	$V_{LSR}^{(2)}$ (km s^{-1})
1	493685.675(7) A	4	8.4(3)	8.15(4)	8.16(4)
2	493720.247(7) A	4	8.6(3)	8.15(4)	8.16(4)
3	494468.182(8) A	4	5.8(2)	8.19(4)	8.11(4)
4	495159.606(8) E	4	6.0(2)	8.17(4)	8.17(4)
5	541986.222(8) A	4	9.7(4)	8.16(4)	8.15(4)
6	542067.209(8) A	4	9.7(4)	8.14(4)	8.15(4)
7	543061.376(12) E	4	6.7(3)	8.18(4)	8.17(4)
8	590261.731(4) A	4	10.5(4)	8.10(4)	8.12(4)
9	590424.408(4) A	4	10.6(4)	8.06(4)	8.14(4)
10	590774.822(7) E	5	7.4(3)	8.19(4)	8.18(4)
11	638262.142(13) E	5	7.5(2)	8.18(3)	8.22(3)
12	638506.307(8) A	4	11.1(3)	8.07(3)	8.08(3)
13	638800.633(8) A	4	11.0(3)	8.07(3)	8.07(3)

matched with model values only in a narrow range of gas densities 1.5×10^7 cm$^{-3} \le n(H_2) \le 1.75\times10^7$ cm^{-3} and kinetic temperatures of 80 K $\le T_{kin} \le$ 100 K. This area is marked by two dotted vertical lines in Fig. 2. As the gas density decreases, $n(H_2) < 1.5\times10^7$ cm^{-3}, the A/E ratio becomes larger than 1, and when $n(H_2) > 1.75 \times 10^7$ cm^{-3} this ratio decreases, and becomes smaller than 1. If one decreases or increases the kinetic temperature inside the selected area, then χ^2 increases dramatically.

The lower panel in Fig. 2 illustrates one of the possible solutions, the position of which is marked with a star on the top panel. The numbers of the methanol lines are plotted along the lower horizontal axis according to Table 2, with the corresponding type of methanol at the top—A or E. The measured peak temperatures and their uncertainty intervals are marked in black, which include systematic temperature scale calibration errors (4% for bands 1a, 1b and 3% for bands 2a [32]) and the average noise amplitude (σ_{rms}). The red color corresponds to the calculated peak temperatures.

The relatively low values of χ^2 in the range of acceptable values of physical parameters reflect the fact that we used major estimates of temperature scale calibration errors. However, this does not affect the main conclusion that the selected A- and E-methanol lines trace the same gas regions with similar physical parameters in the molecular complex Sgr B2(N).

4. ESTIMATES OF $\Delta\mu/\mu$

To perform differential measurements of the fundamental physical constant μ, it is necessary to have pairs of methanol lines with different sensitivity coefficients Q_i, Q_j and measured radial velocities $V_i^{(k)}$, $V_j^{(k)}$ [6]:

$$(\Delta\mu/\mu) \equiv (\mu_{obs} - \mu_{lab})/\mu_{lab} = (V_i^{(k)} - V_j^{(k)})/[c(Q_j - Q_i)], \quad (2)$$

where $c = 299792.458$ km s^{-1} is the speed of light, $k = 1$ or 2 if laboratory or calculated frequencies are used, respectively.

In order to avoid the various systematic errors mentioned in Section 2, we compared sets of lines that fall into the same subrange. In addition, to avert the correlation in errors of $\Delta\mu/\mu$ (see [27, 40]), we use the average values of radial velocities for lines with similar coefficients Q. In Table 5 this is marked on the top panel: the designations V_1 and V_2 indicate the radial velocities of the lines being compared, and the numbers under these designations indicate for which lines the average value was calculated (the numbering corresponds to Table 1). For example, writing 1 + 2 means that the average velocity was calculated from the radial velocities of lines *1* and *2*. The average values of the sensitivity coefficients of the compared lines Q_1 and Q_2 are shown below. In Table 5 the average velocities using both laboratory and calculated frequencies are given, and the corresponding calculated values of $\Delta\mu/\mu$ in units of 10^{-7} are shown as well. This table also shows weighted mean estimates of $\langle\Delta\mu/\mu\rangle^{(k)}$ obtained using laboratory ($k = 1$) or calculated ($k = 2$) reference frequencies.

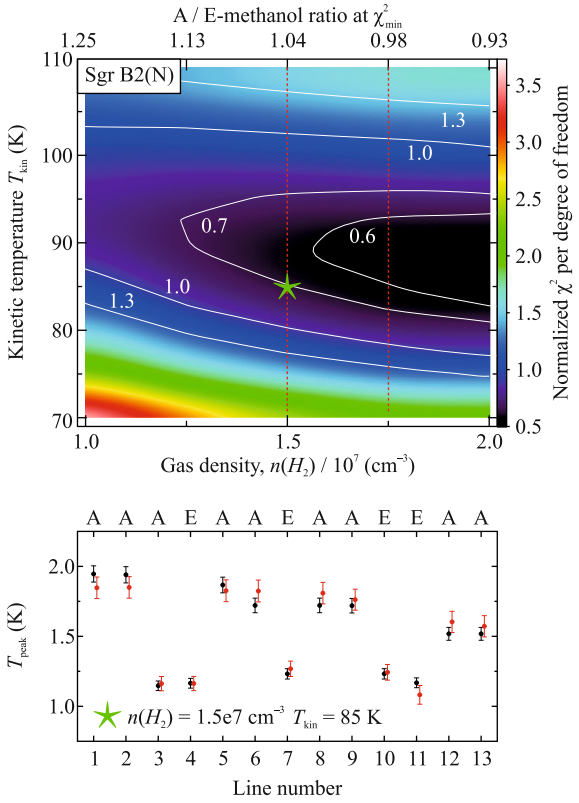

Fig. 2. (Colored online) (Top panel) Map of normalized minimum values of χ^2_{min} as a function of gas density $n(H_2)$ and kinetic temperature T_{kin} at different values of column densities N_A and N_E. Vertical dotted lines limit the range of acceptable values of A/E. The point is marked with a star $\{n(H_2), T_{kin}, N_A, N_E\} = \{1.5e7,\ 85,\ 1.96e15,\ 1.86e15\}$. (Bottom panel) Example of calculated and observed peak temperatures (red and black, respectively) for the thirteen methanol lines from Table 3 at the point marked with the star in the upper panel. The minimum values of χ^2 at this point are as follows: $\chi^2_A = 0.7$, $\chi^2_E = 0.8$, and $\chi^2_{A+E} = 0.7$.

The weighted mean estimates of $\langle\Delta\mu/\mu\rangle^{(k)}$ were calculated using the method of processing an unequal accuracy data set [41]. For Sgr B2(N) in the central part of the Galaxy $\langle\Delta\mu/\mu\rangle^{(1)} = (-4.1 \pm 0.6)\times10^{-7}$ (6.8σ C.L.),[4] if laboratory frequency measurements are used, or $\langle\Delta\mu/\mu\rangle^{(2)} = (-3.5 \pm 0.5)\times10^{-7}$ (7σ C.L.), if calculated frequencies are used instead of laboratory ones. In any case, the result indicates a reduced value of μ with a high level of statistical significance. In this case, the κ, parameter indicating the presence of unaccounted-for systematic errors in the sample or misses at $\kappa > 2$ (equation (4.138) in [41]), in our case equal to 1.17 and 0.98 for the first and second the samples $\Delta\mu/\mu$, respectively.

[4] C.L. means confidence level.

At the same time, for Orion-KL, which is an object far from the Galactic Center, $\langle\Delta\mu/\mu\rangle^{(1)} = (-1.4 \pm 0.6) \times 10^{-7}$ (2.3σ C.L.) according to laboratory frequencies and $\langle\Delta\mu/\mu\rangle^{(2)} = (-1.1 \pm 0.8)\times10^{-7}$ (1.4σ C.L.) if calculated frequencies are utilized. The obtained results for Orion-KL show only the upper limit on the variation of μ at the level of $\Delta\mu/\mu < (6–8)\times10^{-8}$.

Presented in Table 5 the $\Delta\mu/\mu$ values based on laboratory methanol frequencies can be combined with similar data from Table 3 in [27], which contains $\Delta\mu/\mu$ measurements from observations at the IRAM 30-m telescope of two regions of Sgr B2(N) and (M). In this case, the sample size increases to $n = 14$ and the following estimates are obtained: $\langle\Delta\mu/\mu\rangle^{(1)} = (-3.4 \pm 0.4) \times 10^{-7}$ (8.5σ C.L.) and $\kappa = 0.13$.

A statistical normality test criterion can be applied to the combined sample of size $n = 14$. For small size samples ($n \sim 10$) the Shapiro–Wilk criterion is considered to be the most effective [42].[5] In our case, $W = 0.94$ and p-value $= 0.36$ at $\alpha = 0.05$, i.e., the sample is close to normal.

Since all the systematic effects known to us have been taken into account in the course of this study, the result obtained in the direction of the Galactic center $\langle\Delta\mu/\mu\rangle^{(1)} = (-3.4 \pm 0.4)\times10^{-7}$ may indicate a possible decrease in the parameter μ compared to its laboratory value. As confirmation of the absence of any systematics, the spectra of the Orion-KL molecular cloud located far from the Galactic Center, were analyzed and no reliable variations of μ have been found.

5. DISCUSSION OF THE RESULTS AND CONCLUSION

Summing up the work done, it is interesting to compare the $\Delta\mu/\mu$ values in the Sgr B2(N), and Orion-KL spectra compare with those obtained earlier for various molecular clouds distributed in the Galactic disk in the range from $R_{GC} \approx 4$ kpc to $R_{GC} \approx 12$ kpc. This comparison is illustrated in Fig. 3, where the points with uncertainty intervals ±1σ show estimates of $\Delta\mu/\mu$, which used various lines of complex organic molecules CH_3OH, $^{13}CH_3OH$ and CH_3CHO. These lines were observed with various ground-based telescopes and at the Herschel space observatory. Two statistical significance zones ±1σ and ±3σ are shaded in light gray and dark gray, respectively, for the regression curve shown in pink. The

[5] The Shapiro–Wilk statistic W lies in the range $0 < W < 1$, the right boundary of which indicates that the data is close to normal. At the same time, in order to have no reason to reject the hypothesis of normality, a given level of significance, for example, $\alpha = 0.05$ (confidence probability 95%) must correspond to the p value > 0.05.

Table 5. Estimates of $\Delta\mu/\mu$ (in units of 10^{-7}) in Sgr B2(N) and Orion-KL along the lines of methanol CH_3OH (see Eq. (2)). Measured average values of radial velocities V_1 and V_2 (in km s^{-1}) are grouped according to Table 2 in four spectral ranges. The numbers of lines with approximately the same sensitivity coefficients are located under the symbols V_1 and V_2, and the average values of the sensitivity coefficients themselves are given in the row below. The 1σ errors in the last digits are shown in parentheses

V_1	V_2	V_1	V_2	V_1	V_2	V_1	V_2
1 + 2	3 + 4	5 + 6	7	8 + 9	10	11	12 + 13
$Q_1 = -0.1$	$Q_2 = 1.65$	$Q_1 = 0.0$	$Q_2 = 1.7$	$Q_1 = 0.1$	$Q_2 = 1.6$	$Q_1 = 1.6$	$Q_2 = 0.1$
Sagittarius B2(N), f_{obs} & f_{lab} *results*							
65.14(21)	65.42(5)	65.12(4)	65.34(6)	65.43(3)	65.61(6)	65.32(10)	65.15(6)
$\Delta\mu/\mu = -5.4 \pm 4.2$		$\Delta\mu/\mu = -4.2 \pm 1.4$		$\Delta\mu/\mu = -3.9 \pm 1.5$		$\Delta\mu/\mu = -3.7 \pm 2.6$	
Weighted mean $\langle\Delta\mu/\mu\rangle^{(1)} = -4.1 \pm 0.6$							
Sagittarius B2(N), f_{obs} & f_{cal} *results*							
65.15(21)	65.38(4)	65.12(3)	65.32(5)	65.47(3)	65.60(5)	65.36(10)	65.16(6)
$\Delta\mu/\mu = -4.4 \pm 4.2$		$\Delta\mu/\mu = -3.9 \pm 1.1$		$\Delta\mu/\mu = -2.9 \pm 1.1$		$\Delta\mu/\mu = -4.4 \pm 2.6$	
Weighted mean $\langle\Delta\mu/\mu\rangle^{(2)} = -3.5 \pm 0.5$							
Orion-KL, f_{obs} & f_{lab} *results*							
8.15(3)	8.18(3)	8.15(3)	8.18(3)	8.08(3)	8.19(4)	8.18(4)	8.07(2)
$\Delta\mu/\mu = -0.5 \pm 0.8$		$\Delta\mu/\mu = -0.5 \pm 1.0$		$\Delta\mu/\mu = -2.3 \pm 1.0$		$\Delta\mu/\mu = -2.6 \pm 0.9$	
Weighted mean $\langle\Delta\mu/\mu\rangle^{(1)} = -1.4 \pm 0.6$							
Orion-KL, f_{obs} & f_{cal} *results*							
8.16(3)	8.14(3)	8.15(3)	8.17(4)	8.13(3)	8.18(4)	8.22(3)	8.07(2)
$\Delta\mu/\mu = 0.4 \pm 0.8$		$\Delta\mu/\mu = -0.4 \pm 1.0$		$\Delta\mu/\mu = -1.2 \pm 1.0$		$\Delta\mu/\mu = -3.4 \pm 0.9$	
Weighted mean $\langle\Delta\mu/\mu\rangle^{(2)} = -1.1 \pm 0.8$							

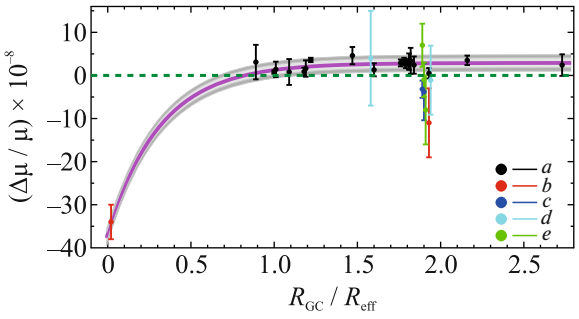

Fig. 3. (Colored online) Measured values of $\Delta\mu/\mu$ along the galactocentric radius R_{GC}, normalized to the effective Galactic radius $R_{eff} \approx 4.5$ kpc. The points with uncertainty intervals ±1σ are taken from the following publications: *a*—[25]; *b*—this work; *c*—[24]; *d*—[9, 11], and *e*—[12], in which the values of $\Delta\mu/\mu$ were estimated along the lines CH_3OH (the first three references), $^{13}CH_3OH$ (the next two references) and CH_3CHO (the last reference). The regression line (pink) is surrounded by the confidence zones ±1σ (light gray) and ±3σ (dark gray).

slight excess of this curve over the zero value of $\Delta\mu/\mu$ depends on the choice of reference frequencies (see Table 4 in [25]) and is not statistically significant. Therefore, the main purpose of such a regression is simply to graphically reflect a sharp change in the value of $\Delta\mu/\mu$ within the interval $0 < R_{GC}/R_{eff} \lesssim 1$.

A similar sharp increase in the circular velocities of stars in the same range of galactocentric distances is observed in our own and other spiral galaxies (e.g., [17, 21, 43]). At the same time, it is generally assumed that in the range of $0 < R_{GC}/R_{eff} \lesssim 1$ there is an increase in the mean density of dark matter against the background of a decrease in the mean density of ordinary baryonic matter, the alignment of ρ_{br} and ρ_{DM} occurs when $R_{GC}/R_{eff} \geq 1$, after which, as R_{GC} increases, dark matter dominates, forming a Galactic halo with a virial mass $M_{vir} \approx 7 \times 10^{11} M_{Sun}$ [43]. In the region of $R_{GC}/R_{eff} \geq 1$ flat stellar rotation curves and zero values of $\Delta\mu/\mu$ are observed at the level of a few 10^{-8}.

In addition, we note that the results of this work limit a number of theoretical models proposed to

explain possible spatial changes in fundamental physical constants. For instance, in theories considering additional scalar fields that trace inhomogeneities of the gravitational field, the change in μ is associated with the gradient of the gravitational potential, $\Delta\mu/\mu = k_\mu \Delta\Phi$ (e.g., [44–46]). This relationship is not confirmed by measurements $\Delta\mu/\mu$ in Sgr B2(N) and Orion-KL, since both molecular complexes have comparable gravitational potentials, $\Phi = GM/c^2r \sim 10^{-9}$ (here r is the radius of the object), but they differ significantly in the estimates of $\Delta\mu/\mu$.

Other models (e.g., [47–49]), which are based on the idea of shielding the fifth force depending on the local density of baryonic matter, which differs by many orders of magnitude between the interstellar medium and its values in terrestrial laboratories, are also not supported by these measurements of $\Delta\mu/\mu$ in Sgr B2(N) and Orion-KL. The local densities of baryonic matter in these clouds are comparable, $n(H_2) \sim 10^7$ cm^{-3}, but the estimates of $\Delta\mu/\mu$ are different.

So, since the $\Delta\mu/\mu$ estimates turn out, as we have shown, to be insensitive neither to the values of the gravitational potential nor to the local density of baryonic matter, the conclusion suggests itself that the detected possible correlation in the distributions of ρ_{DM}/ρ_{br} and $\Delta\mu/\mu$ along the Galactic disk may be related to the density of dark matter. Moreover, if dark matter modulates the Higgs scalar field, then spatial changes in μ can be expected. A similar scenario has been considered, for example, in multidimensional Kaluza–Klein models in [50].

In conclusion, we list the main results obtained in this work.

(1) Processing of two identical sets of high-frequency methanol lines (490–640 GHz) in the spectra of two molecular clouds Sgr B2(N) and Orion-KL show the systematic shifts of these lines relative to each other in the first case, and the absence in the second.

(2) Interpretation of this behavior of line frequencies in terms of small μ-variations, taking into account all systematic corrections, leads to the following mean values: $\langle\Delta\mu/\mu\rangle = (-3.4 \pm 0.4)\times10^{-7}$ for Sgr B2(N) and (M) and $\langle\Delta\mu/\mu\rangle = (-1.1 \pm 0.8)\times10^{-7}$ for Orion-KL.

(3) It is shown using the RADEX code that the A- and E-methanol lines in Sgr B2(N) trace the same gas with the parameters $n(H_2) \approx 1.5\times10^7$ cm^{-3}, $T_{kin} \approx 85$ K, $N_A \approx 2\times10^{15}$ cm^{-2} and the A/E abundance ratio $A/E \approx 1$ expected for hot gas.

(4) A comparison of the distribution of $\Delta\mu/\mu$ values along the galactocentric radius with flat rotation curves of stars in the Galaxy demonstrates a similar nature of these two distributions with a sharp increase in the density of dark matter within the range $0 < R_{GC}/R_{eff} \lesssim 1$ and the same sharp change in the value of $\Delta\mu/\mu$ in the same range. Such a correlation may indicate dark matter modulation of the Higgs scalar field.

ACKNOWLEDGMENTS

The authors would like to thank both anonymous referees for their constructive comments.

FUNDING

This work was supported by the Ministry of Science and Higher Education of the Russian Federation, state assignment no. FFUG-2024-0002 with the Ioffe Institute.

CONFLICT OF INTEREST

The authors of this work declare that they have no conflicts of interest.

REFERENCES

1. J. L. Neill, E. A. Bergin, D. C. Lis, et al., "Herschel observations of extraordinary sources: Analysis of the Herschel/HIFI molecular line survey of Sagittarius B2(N)," Astrophys. J. **789**, 8 (2014).
2. E. A. C. Mills, J. Corby, A. R. Clements, N. Butterfield, P. A. Jones, M. R. Cunningham, and J. Ott, "A centimeter-wave study of methanol and ammonia isotopologues in Sgr B2(N): Physical and chemical differentiation between two hot cores," Astrophys. J. **869**, 121 (2018).
3. J. J. Bernal, C. D. Sophus, and L. M. Ziurys, "Methanol at the edge of the Galaxy: New observations to constrain the galactic habitable zone," Astrophys. J. **922**, 106 (2021).
4. J. Braine, Y. Sun, Y. Shimajiri, F. F. S. van der Tak, M. Fang, Ph. André, H. Chen, and Y. Gao, "Dense gas and star formation in the outer Milky Way," Astron. Astrophys. **676**, A27 (2023).
5. M. G. Kozlov and S. A. Levshakov, "Microwave and submillimeter molecular transitions and their depen-

dence on fundamental constants," Ann. Phys. **525**, 452 (2013).

6. S. A. Levshakov, M. G. Kozlov, and D. Reimers, "Methanol as a tracer of fundamental constant," Astrophys. J. **738**, 26 (2011).
7. P. Jansen, L.-H. Xu, I. Kleiner, W. Ubachs, and H. L. Bethlem, "Methanol as a sensitive probe for spatial and temporal variations of the proton-to-electron mass ratio," Phys. Rev. Lett. **106**, 100801 (2011).
8. J.-P. Uzan, "Fundamental constants: From measurement to the universe, a window on gravitation and cosmology," Living Rev. Relativ. **26**, 6 (2025).
9. J. S. Vorotyntseva, M. G. Kozlov, and S. A. Levshakov, "Methanol isotopologues as a probe for spatial and temporal variations of the electron-to-proton mass ratio," Mon. Not. R. Astron. Soc. **527**, 2750 (2024).
10. J. S. Vorotyntseva, S. A. Levshakov, and M. G. Kozlov, "Spectroscopic shifts in deuterated methanol induced by variation of m_e/m_p," Phys. Rev. A **110**, 012802 (2024).
11. J. Vorotyntseva and S. Levshakov, "Torsion-rotational transitions in methanol as a probe of fundamental physical constants—electron and proton masses," JETP Lett. **119**, 649 (2024).
12. J. S. Vorotyntseva, S. A. Levshakov, and M. G. Kozlov, "Acetaldehyde as a molecule for testing variations of electron-to-proton mass ratio," Phys. Rev. A **113**, 012821 (2026).
13. X. Calmet, "Cosmological evolution of the Higgs boson's vacuum expectation value," Eur. Phys. J. C **77**, 729 (2017).
14. Y. Sofue, M. Honma, and T. Omodaka, "Unified rotation curve of the galaxy—decomposition into de Vaucouleurs bulge, disk, dark halo, and the 9-kpc rotation dip," Publ. Astron. Soc. Jpn. **61**, 227 (2009).
15. F. Nesti and P. Salucci, "The dark matter halo of the Milky Way, AD 2013," J. Cosmol. Astropart. Phys., No. 07, 016 (2013).
16. M. Portail, O. Gerhard, C. Wegg, and M. Ness, "Chemodynamical modelling of the galactic bulge and bar," Mon. Not. R. Astron. Soc. **465**, 1621 (2017).
17. N. G. de Isídio, K. Menéndez-Delmestre, T. S. Gonçalves, M. Grossi, D. C. Rodrigues, N. Garavito-Camargo, A. Araujo-Carvalho, P. P. B. Beaklini, Y. Cavalcante-Coelho, A. Cortesi, L. H. Quiroga-Nuñez, and T. Randriamampandry, "Dark matter distribution in Milky Way analog galaxies," Astrophys. J. **971**, 69 (2024).
18. T. Totani, "20 GeV halo-like excess of the Galactic diffuse emission and implications for dark matter annihilation," J. Cosmol. Astropart. Phys., No. 11, 080 (2025).
19. T. C. Licquia, and J. A. Newman, "Improved estimates of the Milky Way's stellar mass and star formation rate from hierarchical Bayesian meta-analysis," Astrophys. J. **806**, 96 (2015).
20. S. Zhou, A. Aragón-Salamanca, M. Merrifield, B. H. Andrews, N. Drory, and R. R. Lane, "Are Milky-Way-like galaxies like the Milky Way? A view from SDSS-IV/MaNGA," Mon. Not. R. Astron. Soc. **521**, 5810 (2023).
21. M. C. Cavalcante-Siviero, K. Menéndez-Delmestre, P. P. B. Beaklini, T. S. Gonçalves, D. C. Rodrigues, N. G. de Isídio, and A. Araujo-Carvalho, "The universality of dark matter density profiles for Milky Way analog galaxies," arXiv: 2511.00241.
22. S. Ellingsen, M. Voronkov, and S. Breen, "Practical limitations on astrophysical observations of methanol to investigate variations in the proton-to-electron mass ratio," Phys. Rev. Lett. **107**, 270801 (2011).
23. S. A. Levshakov, D. Reimers, C. Henkel, B. Winkel, A. Mignano, M. Centurión, and P. Molaro, "Limits on the spatial variations of the electron-to-proton mass ratio in the galactic plane," Astron. Astrophys. **559**, A91 (2013).
24. M. Daprà, C. Henkel, S. A. Levshakov, K. M. Menten, S. Muller, H. L. Bethlem, S. Leurini, A. V. Lapinov, and W. Ubachs, "Testing the variability of the proton-to-electron mass ratio from observations of methanol in the dark cloud core L1498," Mon. Not. R. Astron. Soc. **472**, 4434 (2017).
25. S. A. Levshakov, I. I. Agafonova, C. Henkel, K.-T. Kim, M. G. Kozlov, B. Lankhaar, and W. Yang, "Probing the electron-to-proton mass ratio gradient in the Milky Way with class I methanol masers," Mon. Not. R. Astron. Soc. **511**, 413 (2022).
26. J. S. Vorotyntseva and S. Levshakov, "Indication of the electron-to-proton mass ratio variation in the Galaxy," JETP Lett. **121**, 589 (2025).
27. J. S. Vorotyntseva, S. Levshakov, and C. Henkel, "Indications of electron-to-proton mass ratio variations in the Galaxy. II. 3 mm methanol lines toward Sgr B2(N) and (M)," JETP Lett. **122**, 715 (2025).
28. https://archives.esac.esa.int/hsa/whsa/.
29. A. Schwörer, Á. Sánchez-Monge, P. Schilke, T. Möller, A. Ginsburg, F. Meng, A. Schmiedeke, H. S. P. Müller, D. Lis, and S.-L. Qin, "The physical and chemical structure of Sagittarius B2. IV. Converging filaments in the high-mass cluster forming region Sgr B2(N)," Astron. Astrophys. **628**, A6 (2019).
30. L. Pagani, C. Favre, P. F. Golgsmith, E. A. Bergin, R. Snell, and G. Melnick, "The complexity of Orion: An ALMA view. I. Data and first results," Astron. Astrophys. **604**, A32 (2017).
31. N. R. Crockett, E. A. Bergin, J. L. Neill, C. Favre, G. A. Blake, E. Herbst, D. E. Anderson, and G. E. Hassel, "Herschel observations of extraordinary sources: Analysis of the HIFI 1.2 THz wide spectral survey toward Orion KL. I. Methods," Astrophys. J. **806**, 239 (2015).
32. D. Teyssier, I. Avruch, S. Beaulieu, J. Braine, A. Marston, P. Morris, M. Olberg, M. Rengel, and R. Shipman, HIFI Handbook, ver.2.1 (2017).
33. L.-H. Xu and F. J. Lovas, "Microwave spectra of molecules of astrophysical interest XXIV: Methanol (CH_3OH and $^{13}CH_3OH$)," J. Phys. Chem. Ref. Data **26**, 1 (1997).
34. L.-H. Xu, J. Fisher, R. M. Lees, H. Y. Shi, J. T. Hougen, J. C. Pearson, B. J. Drouin, G. A. Blake, and R. Braakman, "Torsion-rotation global analysis of the first three torsional states (vt = 0, 1, 2) and terahertz database for methanol," J. Mol. Spectrosc. **251**, 305 (2008).

35. I. M. Avruch, "Cycle38 frequency calibration tests," Tech. Rep. HIFI-ICC-TN-2015-002 (SRON, Groningen, 2011).
36. W. H. Press, S. A. Teukolsky, W. T. Vetterling, and B. P. Flannery, *Numerical Recipies in C* (Cambridge Univ. Press, Cambridge, 2002), p. 693.
37. E. S. Wirström, W. D. Geppert, Å. Hjalmarson, C. M. Persson, J. H. Black, P. Bergman, T. J. Millar, M. Hamberg, and E. Vigren, "Observational tests of interstellar methanol formation," Astron. Astrophys. **533**, A24 (2011).
38. F. F. S. van der Tak, J. H. Black, F. L. Schöier, D. J. Jansen, and E. F. van Dishoeck, "A computer program for fast non-LTE analysis of interstellar line spectra. With diagnostic plots to interpret observed line intensity ratios," Astron. Astrophys. **468**, 627 (2007).
39. D. Rabli and D. R. Flower, "The rotational structure of methanol and its excitation by helium," Mon. Not. R. Astron. Soc. **406**, 95 (2010).
40. S. A. Levshakov, P. Molaro, A. V. Lapinov, D. Reimers, C. Henkel, and T. Sakai, "Searching for chameleon-like scalar fields with the ammonia method," Astron. Astrophys. **512**, A44 (2010).
41. T. A. Agekyan, *Fundamentals of Error Theory for Astronomers and Physicists* (Nauka, Moscow, 1972), p. 144 [in Russian].
42. S. S. Shapiro and M. B. Wilk, "Analysis of variance test for normality," Biometrika **52**, 591 (1965).
43. A.-C. Eilers, D. W. Hogg, H.-W. Rix, and M. K. Ness, "The circular velocity curve of the Milky Way from 5 to 25 kpc," Astrophys. J. **871**, 120 (2019).
44. J. Magueijo, J. D. Barrow, and H. Sandvik, "Is it *e* or is it *c*? Experimental tests of varying alpha," Phys. Lett. B **549**, 284 (2002).
45. V. V. Flambaum and E. V. Shuryak, in *Nuclei and Mesoscopic Physics,* Ed. by P. Danielewicz, P. Piecuch, and V. Zelevinsky, AIP Conf. Proc. **995**, 1 (2008).
46. S. Blatt, A. D. Ludlow, G. K. Campbell, et al., "New limits on coupling of fundamental constants to gravity using ^{87}Sr optical lattice clocks," Phys. Rev Lett. **100**, 140801 (2008).
47. J. Khoury and A. Weltman, "Chameleon fields: Awaiting surprises for tests of gravity in space," Phys. Rev. Lett. **93**, 171104 (2004).
48. K. F. Olive and M. Pospelov, "Environmental dependence of masses and coupling constants," Phys. Rev. D **77**, 043524 (2008).
49. P. Brax, "An environmental variation of constants," Phys. Rev. D **90**, 023505 (2014).
50. A. Carmona, J. C. Ruiz, and M. Neubert, "A warped scalar portal to fermionic dark matter," Eur. Phys. J. C **81**, 58 (2021).

Translated by the authors